Chapter 1

1.   INTRODUCTION

This chapter provides a comprehensive overview on synthesis and applications of metal oxide-based nanostructures. The suitable synthesis protocols for the fabrication of metal oxide-based nanostructures have also been outlined herein. The technological developments in the design and synthesis of metal-oxide based nanostructures over the years is studied with emphasis on achieving material's property for advanced applications. At the end of the chapter, the objectives of each chapter of the thesis have been presented.

1.1   Background

Nanotechnology constitutes one of the six "Key Enabling Technologies" recognized by the European Commission [1]. Although the concept of nanotechnology is quite recent, its development can be traced to the early medieval period when artisans created stained glass windows with the incorporation of silver and gold nanoparticles into glass in its molten state [2]. The theory and concepts underlying nanotechnology unfolded with a talk entitled "There's Plenty of Room at the Bottom" presented by renowned physicist Richard P. Feynman at an American Physical Society meeting held at Caltech in 1959 [3]. In his lecture, Feynman asked the question "Why cannot we write the entire 24 volumes of the Encyclopedia Britannica on the head of a pin?". He proposed that manipulation of individual atoms and molecules might be possible using one set of precise tools to build and operate another proportionally smaller set, scaling down to the needed scale [4]. Fifteen years later, Professor Norio Taniguchi from Tokyo University of Science first defined the term "nanotechnology" in 1974 as "Nanotechnology mainly consists of the processing of separation, consolidation, and deformation of materials by one atom or by one molecule" [5]. However, something as tiny as a nanoparticle is impossible to view with the naked eye and light microscope. The advent of scanning tunnelling microscope followed by the atomic force microscope provided scientists with the necessary instruments, ushering in the age of nanotechnology [6]. In 1986, Dr. K. Eric Drexler published his book "Engines of Creation: The Coming Era of Nanotechnology" and popularized the idea of nanotechnology [7]. Subsequently, the first issue of "Nanotechnology" journal was launched in 1990 [8]. Concomitantly, the interest in carbonaceous materials increased after the structure elucidation of carbon nanotube by Sumio Ijima [9]. In 1996, Robert F.

Curl, Harold W. Kroto and Richard E. Smalley were awarded the Nobel Prize in Chemistry for the discovery of fullerenes in 1985 [10]. Since the beginning of the 21st century, interest in the fields of nanoscience and nanotechnology has increased considerably. Starting from the launch of National Nanotechnology Initiative (NNI) to the application of nanoparticles in drug delivery, nanotechnology has taken the global market by storm [11]. Figure 1.1 displays the timeline of breakthrough developments in the field of nanotechnology.
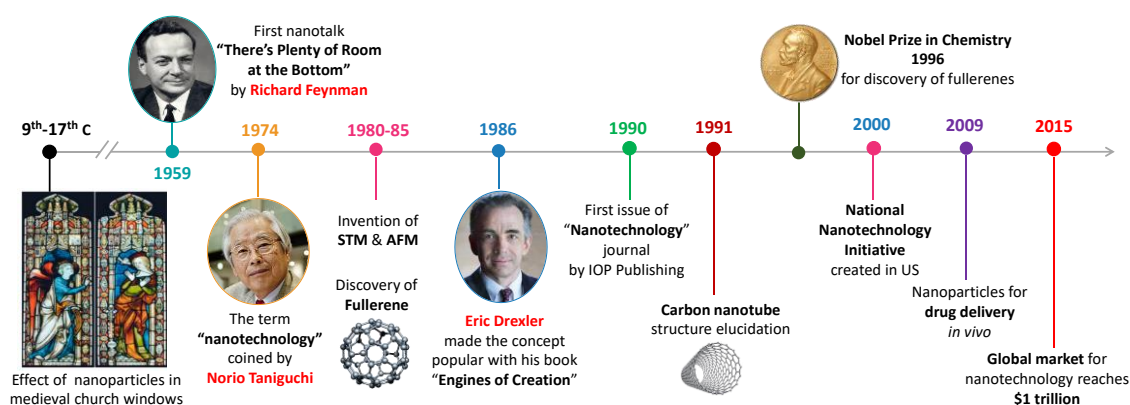

Figure 1.1 Timeline of breakthrough developments in the field of nanotechnology.

1.2   Nanomaterials

Nanomaterials are conventionally defined as materials possessing at least one dimension in the range of 1 to 100 nm [12]. Nanotechnology is an excellent example of an emerging technology which deals with engineered nanomaterials exhibiting substantially enhanced performances [13]. Nanomaterials show different physicochemical properties compared to their bulk counterparts. In general, the quantum confinement of electrons by the potential wells of nanomaterials has been considered as one of the most powerful components in controlling their unique properties [14]. Additionally, the unique characteristics are related to different aspects such as:

(1)   Large fraction of surface atoms,

(2)   Large surface energy,

(3)   Spatial confinement, and

(4)   Reduced imperfections.

The properties of nanostructured materials are tunable by altering their size, shape and/or extent of agglomeration. Table 1.1 depicts few instances of adjustable properties of nanomaterials suggested by G. Cao [15].

Table 1.1 Adjustable properties of nanomaterials with examples.

Property	Example
Catalytic	Better catalytic efficiency through a higher surface-to-volume ratio
Mechanical	Improved mechanical strength owing to reduced probability of defects
Optical	The spectral shift of optical absorption of metallic nanoparticles with their varying size, attributable to surface plasmon resonance
Electrical	Improved electrical conductivity with better ordering in microstructure; Decreased electrical conductivity due to reduced dimension and increased surface scattering
Magnetic	Superparamagnetic behavior owing to huge surface energy

1.2.1   Classification of nanomaterials

Nanomaterials can be classified into four types based on their dimensionality [16].

(i)   Zero-dimensional (0D) nanomaterials: These materials have all three dimensions within the nanoscale (i.e., <100 nm). Examples of 0D nanomaterials include quantum dots, fullerenes, atomic clusters, metal oxide nanoparticles etc. Due to their ultra-small size, quantum confinement effect, optical stability, cell permeability and biocompatibility, 0D nanomaterials have demonstrated great potential for optoelectronic and biomedical applications [16].

(ii)   One-dimensional (1D) nanomaterials: These materials have one dimension outside the nanoscale (i.e., >100 nm). Examples of this type include nanorods, nanowires and nanotubes. 1D nanomaterials exhibit excellent electron mobility and high mechanical strength which make them potential candidates for nanodevices, optoelectronic materials, catalysis and photocatalysis.

(iii) Two-dimensional (2D) nanomaterials: In 2D nanomaterials, two of their dimensions lie outside the nanoscale. They have plate-like structures in different forms such as nanosheets, nanoflakes, nanolayers and so on, with thickness of at least one atomic layer. Some examples of 2D nanomaterials are layered double hydroxides, graphene, graphene oxide, reduced graphene oxide, silicate clays, graphitic carbon nitride etc. [17]. 2D nanomaterials have been extensively utilized in several applications such as drug delivery, biosensors, multimodal imaging, catalyst supports and so forth due to their high surface-to-volume ratio and surface charge [18].

(iv) Three-dimensional (3D) nanomaterials: These are materials with all the three dimensions outside the nanoscale. In other words, 3D nanomaterials are not restricted to nanoscale in any dimension. These materials possess arrangements of multiple nanosized crystals with different orientations [19]. They exhibit unique features such as high surface area, improved mechanical strength and charge transfer. 3D nanomaterials include bulk powders, bundles of nanowires and nanotubes, multi-nanolayers, dispersed nanoparticles, 3D hierarchical nanostructures and so forth [20]. It has been observed that 3D nanomaterials are the most abundant nanomaterials in commercialized products which are currently present in 78% of all nanoproducts [21]. Figure 1.2 illustrates the classification of nanomaterials according to their dimensionality.
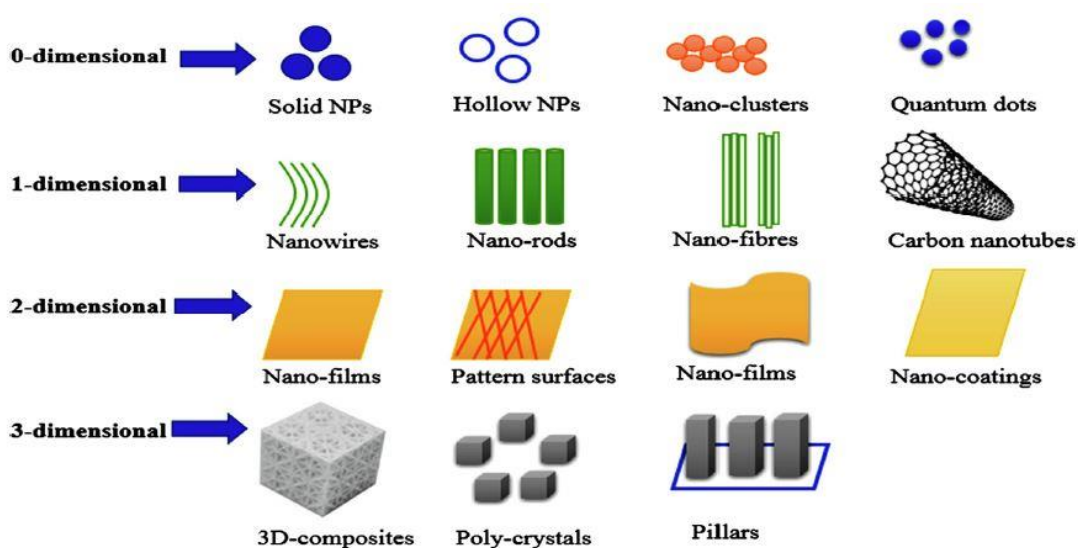

Figure 1.2 Classification of nanomaterials based on dimensionality. [Reproduced from 22]

1.3   Metal oxides

Metal oxides represent a class of inorganic compounds that play significant role in different areas of physics, chemistry, and materials science [23, 24]. They can adopt a variety of structural geometries that exhibit metallic, semiconductor or insulator behavior [25]. The physicochemical properties of metal oxides have attracted the interest of researchers as these are sensitive to changes in size, composition, structure, native defects, doping etc. [26]. Due to their high surface area, porosity, ease of separation, chemical and thermal stability, metal oxides are widely used as active phase, support, and promoter for various industrial applications [25, 26]. Moreover, metal oxides have been utilized in heterogeneous catalysis owing to their acid-base and redox properties [23]. The principal catalytic domains of metal oxides cover acid and base catalysis, oxidation reactions, photocatalysis, and biomass conversion [24]. They are also employed as sorbents for removal of harmful CO, NO_x, and SO_x species formed during combustion of fossil-derived fuels [27]. Moreover, the tunable band gap and electronic structure of metal oxides results in a wide range of applications in microelectronic circuits, sensors and optoelectronic devices [25].

1.3.1   Zinc oxide and tin dioxide

Among the various metal oxides, zinc oxide (ZnO) and tin dioxide (SnO_2) are promising materials because of their distinctive conductance properties, acid-base properties and process flexibility [28]. Therefore, it is necessary to understand their structure and properties before studying in reduced dimensions. The structure and properties of ZnO and SnO_2 are addressed in the following sections.

1.3.1.1 Structure of zinc oxide (ZnO) and tin dioxide (SnO_2)

ZnO crystallizes in three different forms: wurtzite, zinc blende and rocksalt structure. Among these, the thermodynamically stable phase at ambient conditions is the hexagonal wurtzite structure having lattice parameters a = b = 3.2495 Å and c = 5.2062 Å. Both Zn^{2+} and O^{2-} ions are tetrahedrally coordinated to each other and stacked alternately along the c-axis [29, 30]. Figure 1.3 represents the structure of ZnO unit cell.
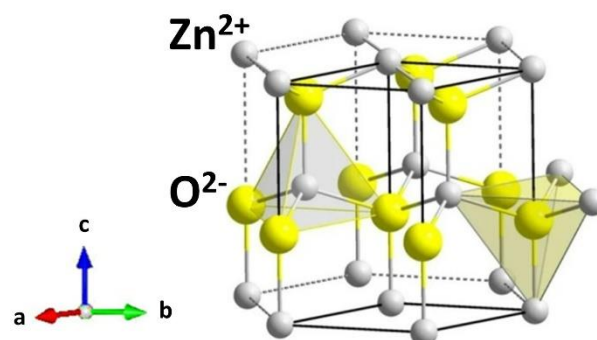
Figure 1.3 Unit cell of ZnO.

SnO$_2$ usually crystallizes in the tetragonal rutile structure. It has a tetragonal symmetry with a = b = 4.737 Å and c = 3.186 Å. Each Sn^{4+} is coordinated to six O^{2-}, and each O^{2-} is coordinated to three Sn^{4+} at the corners of an almost equilateral triangle. Figure 1.4 represents the structure of SnO$_2$ unit cell. A pressure-driven sequential transition to other possible polymorphs such as rutile-type, CaCl$_2$-type, α-PbO$_2$-type, pyrite-type, ZrO$_2$-type orthorhombic phase I, fluorite-type and cotunnite-type orthorhombic phase II has also been reported for SnO$_2$ [31].
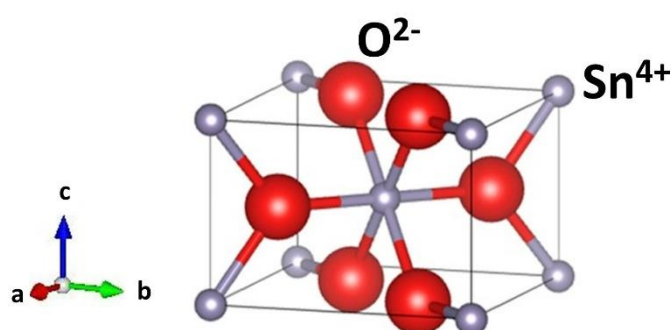

Figure 1.4 Unit cell of SnO$_2$.

1.3.1.2 Properties of zinc oxide and tin dioxide

ZnO is an n-type wide band gap (3.37 eV) semiconductor with high exciton binding energy (60 meV) [32]. Due to its biocompatibility, low-toxicity and inexpensive nature, ZnO with its unique properties are employed in several applications such as catalysis, photocatalysis, antibacterial treatments, cosmetics, UV absorption etc. [32–36]. Some of the salient properties of ZnO have been mentioned in Table 1.2.

Tin dioxide (SnO_2) is also an n-type wide band gap (3.6 eV) semiconductor [31]. Owing to its good electrical, optical, electrochemical and redox properties, SnO_2 has been employed in solar cells, catalysis, chemical sensors and high-capacity lithium-storage [37–40]. Some of the key properties of SnO_2 are also listed in Table 1.2.

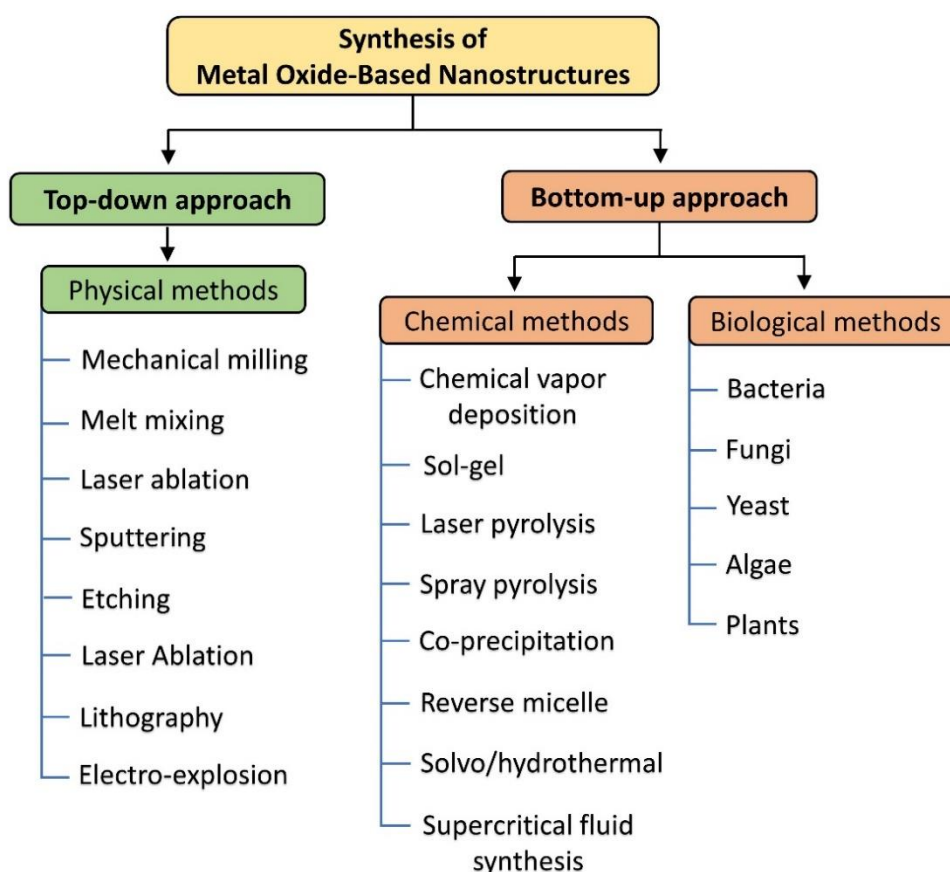**Table 1.2** Some key properties of ZnO [32] and SnO_2 [31].

Entry	Property	ZnO	SnO$_2$
1	Molar Mass	81.38 g/mol	150.71 g/mol
2	Crystal structure	Wurtzite	Rutile
3	Space group	$P6_3mc$	$P4_2/mnm$
4	Density	5.61 g/cm^3	6.95 g/cm^3
5	Melting point	1975 °C	1630 °C
6	Boiling point	2360 °C	1800-1900 °C
7	Band gap	3.37 eV	3.6 eV
8	Exciton binding energy	60 meV	130 meV
9	Solubility in water	Insoluble	Insoluble
10	Solubility	Soluble in dilute acids and bases	Soluble in conc. H_2SO_4 and HCl

1.4 Metal oxide-based nanostructures

In recent years, metal oxide-based nanostructures have stimulated great research interest due to their fascinating physicochemical properties [41]. The spatial confinement of these nanostructures along with other surface characteristics, such as high surface energy and strong surface adsorption, are advantageous. They also possess large surface-to-volume ratio, porosity and defect centers that significantly improve their performance in various applications. These novel properties of metal-oxide based nanostructures can be modified by fabricating nanostructures with varying morphologies [42]. Therefore, the primary focus of nanotechnology lies in the synthesis of nanostructures or nanoarrays having distinctive properties compared to bulk or single particle species [25].

1.4.1 Synthesis of metal-oxide based nanostructures

Several methods have been utilized for the synthesis of oxide nanostructures till date [43, 44]. The synthesis of nanostructured materials is generally divided into two categories: (i) top-down approach and (ii) bottom-up approach. Scheme 1.1 depicts the various methods under these two approaches for the synthesis of oxide nanostructures.

Synthesis of Metal Oxide-Based Nanostructures

Top-down approach

Physical methods
— Mechanical milling
— Melt mixing
— Laser ablation
— Sputtering
— Etching
— Laser Ablation
— Lithography
— Electro-explosion

Bottom-up approach

Chemical methods
— Chemical vapor deposition
— Sol-gel
— Laser pyrolysis
— Spray pyrolysis
— Co-precipitation
— Reverse micelle
— Solvo/hydrothermal
— Supercritical fluid synthesis

Biological methods
— Bacteria
— Fungi
— Yeast
— Algae
— Plants

Scheme 1.1 Various methods of synthesis of oxide nanostructures.

The top-down approach involves those preparative methods where nanometer sized materials are obtained by physically breaking down bigger building blocks. On the other hand, the bottom-up approach is based on building up of nanostructured materials from atomic or molecular precursors [44]. This approach is of significant interest compared to the top-down approach due to the possibilities of manipulating the properties of the final nanostructured materials [43]. It provides the ability to control several properties, viz. size, shape, stoichiometry, surface area and pore size of nanostructures. Among the various methods classified under bottom-up approach (Scheme 1.1), the solvo/hydrothermal methods that favor shape control have been

considered easy, simple and powerful. The hydrothermal synthesis crystallizes substances at high vapor pressure from high-temperature aqueous solutions [45–48]. The crystal growth is achieved in a special stainless steel pressure vessel called autoclave, wherein a nutrient is added along with water. A gradient of temperature is retained at both ends of the growth chamber. The hotter end dissolves the nutrient and the cooler end causes seeds to take additional growth [48]. The solvothermal method is similar to hydrothermal method except that here crystal is synthesized in the presence of various organic solvents. The use of variety of organic solvents having different properties offers room for new materials [46]. The key advantage of solvo/hydrothermal methods is the ability to grow crystalline phases that are otherwise unstable at their melting points. Materials having high vapor pressure near their melting points are also grown by these methods. Moreover, these methods are based on the features of easy control and large-scale fabrication.

1.4.2   Supported metal oxide-based nanostructures

Now-a-days, the uses of supported metal oxide-based nanostructures have attracted great attention. The nanostructured metal oxides immobilized on solid supports remain insoluble in solvents thereby preventing them from leaching or aggregation during catalysis [49]. Several supports such as silica, zeolites, carbon-based materials etc. are used in different reactions. There are various advantages of using supports such as reduced cost, high activity and reusability. The support aids the active phase, i.e., metal/metal oxide synergistically to perform better in a chemical reaction. For instance, the support material changes the electron density of the supported metal nanoparticle, turning chemically inert gold into an efficient catalyst [50]. The redox, acid-base, conductive properties and porous nature of supports play a key role in designing effective catalysts [51, 52]. A suitable support material should possess distinguished properties such as

      (1) Chemical inertness,

      (2) Resistance to high temperatures, acids and bases,

      (3) Large surface area,

      (4) Mechanical robustness,

      (5) Thermal stability and

      (6) Good ligation to the metal/metal oxide

For synthesizing catalysts over suitable support materials, two methods are widely followed: (i) co-precipitation method and (ii) impregnation method. Co-precipitation method employs the addition of a precipitating agent to the catalytically active component with the precipitate being held by the support material. This approach is relatively simpler for synthesis but ineffective for controlling the shape and morphology of the material. In the impregnation method, the pores of the support material are filled by the active material in a solvent and the solvent is eventually evaporated. Interaction between the support and the active material exists in this method which may be suitable for controlling the catalyst's dispersion over the support [50, 51].

1.4.3   Doped metal oxide-based nanostructures

The demands for metal oxide-based nanostructures have been rapidly increasing in the field of photocatalysis [52]. An important feature of photocatalyst is its ability to absorb light efficiently. Nevertheless, the wide band gap of metal oxides limits their absorption to ultraviolet region. Therefore, the band gaps of metal oxides have been engineered by inclusion of dopants into its lattice [53]. Doping induces changes to the metal's crystal and electronic structure, resulting in band gap alterations [54]. The doping of ions creates band states in between the energy gap of the metal oxide and extends its absorption edge towards visible region [55]. Both metals and non-metals can be utilized as dopants for modifying the band gap of metal oxide nanostructures [56]. In case of non-metals such as carbon, nitrogen, phosphorus, etc., their 2p orbitals introduce localized states near the edges of the valence and/or conduction bands leading to band gap narrowing and subsequently improving visible light response [57]. However, high percentages of doping can generate recombination centers which lowers the amount of active charge carriers [58]. Metal dopants, on the other hand, can also reduce the band gap of metal oxides and improve their performances [59]. In this case, 3d orbitals of the metal introduce electronic states within the original band gap of the metal oxide [60].

1.4.4   Applications of metal oxide-based nanostructures

Metal oxide-based nanostructures have received considerable importance during the past two decades due to their potential applications in various chemical and industrial processes. This is evidenced from the rise in the number of publications on "Applications of metal oxide nanostructures" as presented in Figure 1.5.
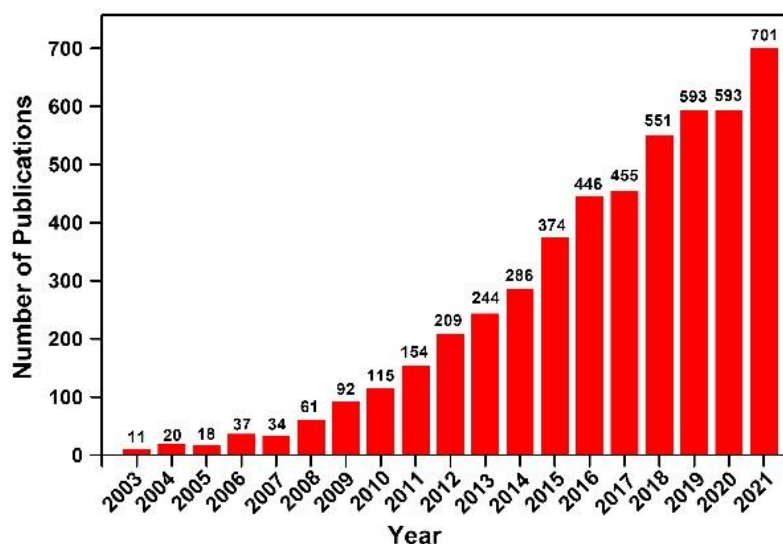
Figure 1.5 Bar plot of number of publications on "Applications of metal oxide nanostructures" (Source: Web of Science). Database survey conducted in November 2022.

The diverse applications of metal oxide-based nanostructures are schematically presented in Figure 1.6. Metal oxide-based nanostructures have been applied in various fields such as organic transformations, wastewater treatment, solar cells, sensors, electrocatalysis and so forth [61-64]. Here, we have mainly focused on applications of metal oxide-based nanostructures in two major fields: (i) organic transformation and (ii) wastewater treatment.
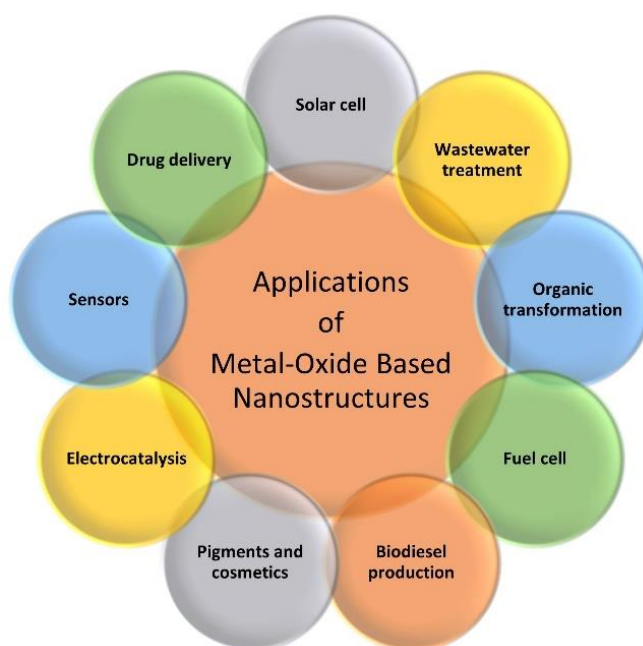

Figure 1.6 Applications of metal oxide-based nanostructures in various fields.

1.4.4.1 Organic transformation

Metal oxide-based nanostructures have been employed as catalysts for various important organic transformations such as cross-coupling reactions, hydroboration reaction, Friedel-Crafts alkylation and acylation reactions, Knoevenagel reaction, epoxidation, chemoselective oxidations and reductions etc. [65, 66]. In general, the products of these transformations are employed as starting substrates for synthesizing specialty chemicals such as pharmaceuticals and agrochemicals [67, 68]. Among them, aromatic ketones are fundamental intermediates in the synthesis of pharmaceuticals, natural products, functional materials and agrochemicals [69]. Out of several organic transformations used for the synthesis of aromatic ketones, the Friedel-Crafts (FC) acylation reaction is considered one of the most efficient methods due to its simplicity and high selectivity [70, 71].
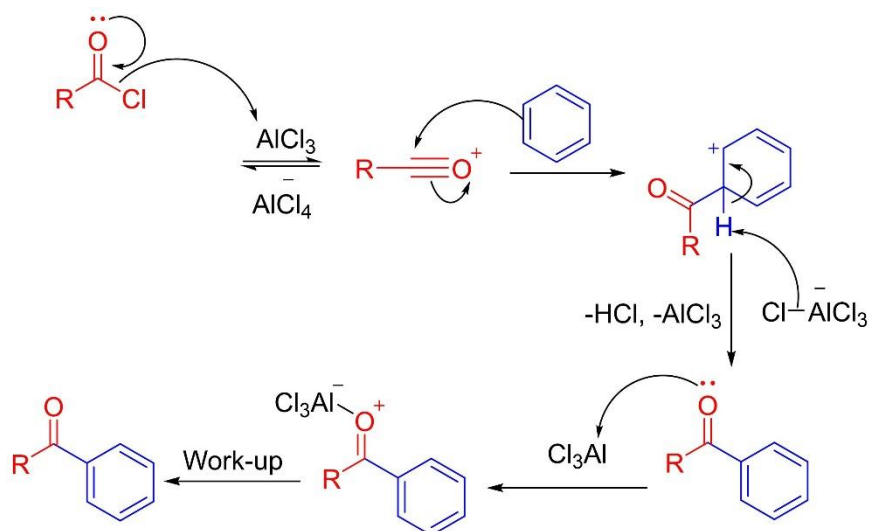
1.4.4.1a   Friedel-Crafts acylation reaction

The Friedel-Crafts acylation reaction is among the oldest reactions for C–C bond formation leading to formation of potent drug molecules and their intermediates such as benzophenone derivatives like terfenadine, cetirizine etc. [72, 73]. A typical Friedel-Crafts acylation reaction involves the electrophilic substitution of an aromatic compound with an acylating agent in the presence of more than 1 equivalent of Lewis acid catalyst (e.g., anhyd. $AlCl_3$) due to its strong complexation with the resultant ketone [74]. Scheme 1.2 represents the FC acylation reaction of aromatic compounds.
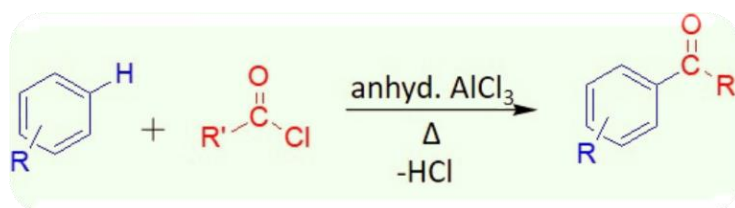
Scheme 1.2 Friedel-Crafts acylation reaction.

The general mechanism for FC acylation reaction is shown in Scheme 1.3. The mechanism is initiated by the reaction of Lewis acid catalyst with the acylating agent (acid chloride/acid anhydride), leading to the formation of an acylium ion. The acylium ion behaves as an electrophile and reacts with the nucleophilic aromatic substrate to form an intermediate complex, thereby destroying the aromatic property of the ring. To regain its aromaticity, deprotonation of the intermediate complex occurs, resulting in the

Scheme 1.3 General mechanism for Friedel-Crafts acylation reaction.

formation of aromatic ketone [75]. The other conventional catalysts for this reaction are Brönsted acids (HF, H_2SO_4, HCl) or other Lewis acid catalysts (anhydrous $FeCl_3$, $ZnCl_2$, $SnCl_2$ etc.) [76, 77]. All these catalytic systems are associated with several drawbacks of handling and recovery, and generates toxic waste. To overcome this issue, various solid acid catalysts, such as zeolites, clays, heteropoly acids, metal oxides, acid treated metal oxides, and so forth, have been developed for the FC acylation reaction [76, 78]. Among them, metal oxides are the prominent solid catalysts due to the presence of numerous edge and corner sites, improved reactivity and selectivity, non-corrosive nature and low-cost [79].

Raula *et al.* [80] synthesized flowerlike zinc oxide (ZnO) nanostructures with ascorbate ion as a shape-directing/capping agent and employed them for the FC acylation reaction of anthracene with benzoyl chloride. They observed different shapes of ZnO nanostructures such as flowerlike, spindlelike, and spherical with increasing synthesis temperature from 60 to 90 °C. Their findings suggested that the flowerlike ZnO nanostructures have slightly higher catalytic activity towards FC reaction than their spherical counterpart. This variation in the activity was assumed to arise from the hyperbranched nature of flowerlike nanostructures. Another possibility is the occurrence of more defect states in the flowerlike ZnO nanostructures than in spherical ZnO. Karim and co-workers [81] demonstrated the use of flower-shaped ZnO nanostructure as a heterogenous catalyst for the solvent less acylation reaction of a naturally occurring product, namely 2,5,9,9-tetramethyl-6,7,8,9-tetrahydro-5H-benzocycloheptene (ar-himachalene) with acid chlorides. According to their results, the aromatic group of ar-

himachalene can be effectively and selectively catalyzed by the ZnO nanoflowers. Furthermore, the catalyst could be recycled up to 3 times by filtration and washing with insignificant loss in its catalytic activity. Hoseini *et al.* [82] investigated the use of Fe_3O_4 nanoparticles (NPs) as efficient catalyst for FC acylation of aromatic compounds. They performed the reaction with acid chlorides at room temperature in solvent-free conditions. Based on the investigation, they reported that the catalyst showed two main advantages in FC acylation reaction: Firstly, the interaction between reactants and catalyst increased significantly due to high surface area of the NPs. Secondly, the Fe_3O_4 NPs could be easily separated from the reaction mixture by applying an external magnet due to their paramagnetic properties and insolubility in the reaction mixture. The recovered catalyst could be reused for successive runs without appreciable loss in its activity.

Li and co-workers [83] reported the synthesis of iron oxide (Fe_2O_3) supported on HY zeolite with varying Si/Al ratio (SAR) for Friedel–Crafts acylation of *m*-xylene. They observed that the synthesized catalyst exhibits excellent catalytic activity for the acylation reaction. The catalytic activity increased with the decrease of SAR of the HY zeolite due to the increase in Lewis acidic sites and the results are presented in Table 1.3. The catalyst was also easily recovered from the reaction mixture and recycled for 5 consecutive runs without considerable loss of activity.

Table 1.3 Effect of Si/Al ratio of HY zeolite to the reaction[a] [83].

Entry	Catalyst	Conversion (%)	Selectivity (%)	Yield (%)
1	Fe_2O_3/HY (Si/Al = 7)	99.58	94.48	93.88
2	Fe_2O_3/HY (Si/Al = 9)	80.63	95.31	76.85
3	Fe_2O_3/HY (Si/Al = 11)	79.39	89.12	70.75

[a]Reaction condition: *m*-xylene : benzoyl chloride = 4 : 1; catalyst dose = 5 wt%; T = 130 °C.

Reddy *et al.* [84] synthesized aromatic ketones via FC reaction over 3D SnO_2−SiO_2 mesoporous composite catalysts. As per their report, the synthesized catalysts were found superior to functionalized MCM-41, modified zeolites and supported heteropolyacid catalysts, with high yield (up to 92%) and regioselectivity. Abedi and co-workers [85] reported the synthesis of zinc oxide (ZnO) nanoparticles dispersed on

polyaniline (PANI) supporting matrix in aqueous medium and employed it for FC acylation reactions. They observed that the PANI/nano-ZnO composites are efficient catalysts for the acylation reactions and could activate the reactant at ambient temperature. Moreover, the catalyst could be reused for five cycles without significant loss in its activity.

Again, microwave-assisted organic transformations have gained special attention in improving organic reactions by providing the shortest and most efficient routes [86]. The main advantage of microwave (MW) heating is its "core heating" mechanism or dipolar mechanism [87]. A substance is microwave active if it possesses some dipole moment. The dipole is sensitive to external electric field and attempts to orient itself with the field's direction [88]. The rapidly oscillating electric field (900–2450 MHz) of MW radiation results in the orientation of dipoles in a reaction mixture, thereby inducing rotation and intermolecular frictions between them [89]. MW heating enables internal core heating to a greater extent compared to conventional heating by the dissipation of MW energy as heat due to these induced rotations. MW irradiation has been successfully applied to FC acylation using different catalytic systems [86, 90-93]. The shortened reaction time with MW irradiation limits the decomposition of reagents and products, promotes chemo- and regioselectivity of isomers and inhibits diacylation [86]. The use of MW irradiation for metal oxide-catalyzed FC acylation is sparse in reports. Pasha *et al.* [94] reported TiO_2-mediated FC acylation of aromatic compounds under MW irradiation. They observed that the acylation proceeded very rapidly within 20-50 sec yielding exclusively para-acylated ketones. Unactivated benzenes such as chlorobenzene also underwent the acylation reaction and afforded acceptable yields (65-70%) of the corresponding aromatic ketone. This finding clearly indicates that the integration of the advantages of MW method and the characteristics of metal oxides can be highly beneficial for enhancing the catalytic activities toward FC acylation reaction.

1.4.4.2 Wastewater treatment

The rapid growth of industries and increasing population have led to inappropriate disposal of toxic wastes/contaminants/chemical pollutants into water bodies. These toxic wastes include organic dyes, pesticides, heavy metals and pharmaceuticals residues [95]. All these contaminants released into the environment need to be eliminated to preserve ecological stability, aquatic biota and human health

[95–97]. Among the chemical pollutants in wastewater, organic dyes due to their toxic nature are one of the major contaminants imposing environmental concern [98]. Therefore, it is of utmost importance to treat these organic dyes from industrial effluents prior to their discharge into the environment. To remove such organic dyes from wastewater, various treatment methods have been developed as shown in Figure 1.7.
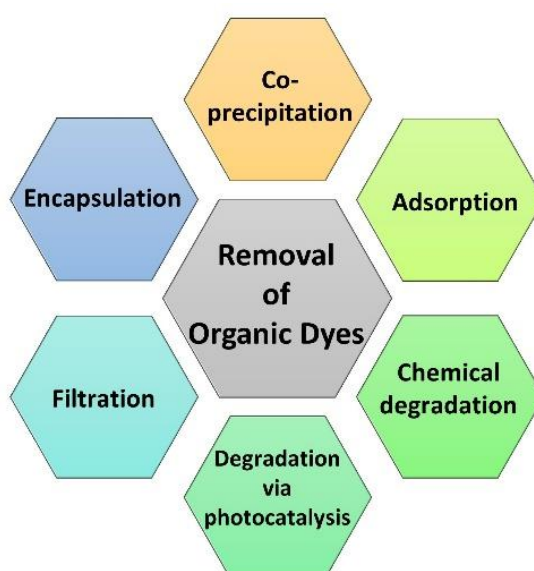

**Figure 1.7** Methods for removal of organic dyes [99].

Among the various methods of dye removal, adsorption and degradation via photocatalysis are superior to other techniques due to

      (1) Eco-friendly nature,

      (2) No secondary pollution, and

      (3) Non-consumption of expensive organic chemicals.

1.4.4.2a   Adsorptive removal of dyes

Adsorption is a surface phenomenon involving the adhesion of atoms, ions or molecules from gas, liquid or dissolved solid to surface of adsorbent [100]. This method is most widely adopted for removing organic contaminants from aqueous solution. Various adsorbents such as activated carbon, zeolites, clays, layered double hydroxides, metal oxide nanostructures, fly ash etc. have been utilized for dye removal [101–104]. Among them, nanostructured metal oxides are considerably used as adsorbent for various organic dye pollutants in wastewater treatment due to their high surface area and porosity [105–107].

Abdelkader *et al.* [108] synthesized SnO_2 NPs with an average size of 13–23 nm via a sol-gel method. Further, it was employed for adsorption of congo red (CR) dye from aqueous solution. The adsorption efficiency was found to be 84.41% which could be attributed to the electrostatic interaction between Sn^{2+} and electron-rich N atoms of CR moiety. Athira *et al.* [109] studied the adsorption of malachite green (MG) from aqueous solution using SnO_2 NPs synthesized via hydrothermal route with adsorption capacity of 118.90 mg/g. The adsorption kinetics indicated that the adsorption of MG onto SnO_2 NPs is controlled by pseudo-second order kinetics. Nazar and co-workers [110] demonstrated the adsorption of two azo dyes, viz., methyl orange (MO) and amaranth (AM) from their aqueous solution using ZnO NPs synthesized by co-precipitation method. The percentage removal for MO and AM was found to be 70.3% and 94.2%, respectively. The kinetics studies indicated that the adsorption of both the dyes onto the ZnO NPs followed pseudo-second order kinetics. Based on their observations, a schematic adsorption-desorption mechanism (Scheme 1.4) was suggested explaining that the adsorption of both the dyes could be due to the electrostatic interaction between negatively charged groups on the anionic dyes and positively charged groups on the ZnO NPs.
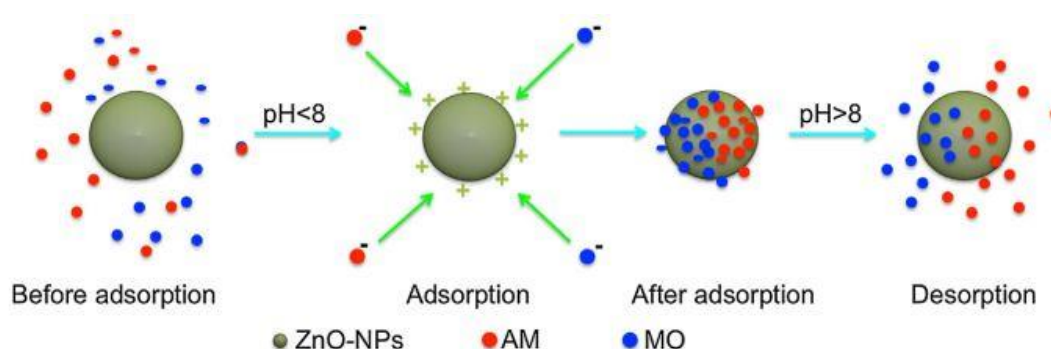
Scheme 1.4 Adsorption-desorption mechanism between ZnO NPs and anionic dyes (MO and AM). [Reproduced from 110]

Verma *et al.* [111] synthesized graphene oxide-manganese dioxide (GO-MnO₂) nanocomposite via hydrothermal route for the adsorptive removal of cationic methylene blue (MB) and anionic methyl orange (MO) dyes from aqueous solution. A removal efficiency of achieved for both MO and MB within the starting 5 min of adsorption are presented in Figure 1.8. Although both the dyes can be removed by the synthesized adsorbent, the extent of MB removal is higher than that of MO. This is attributed to the greater interaction between existing opposite charges on GO-MnO₂ and MB compared to

that of MO. The kinetics studies revealed that the adsorption of both the dyes (MO and MB) onto the GO-MnO$_2$ nanocomposite followed pseudo-second order kinetic model.
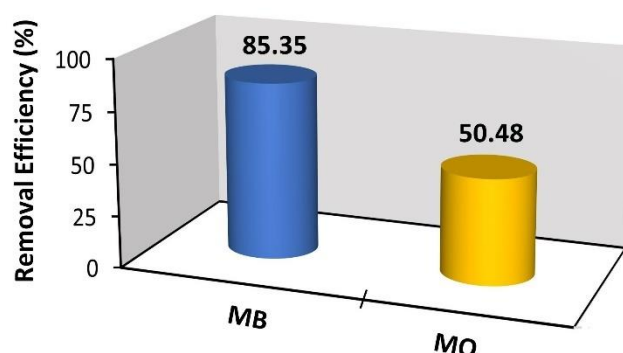

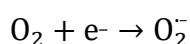
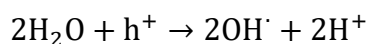**Figure 1.8** Removal efficiency (%) of dyes on GO-MnO$_2$ nanocomposite.

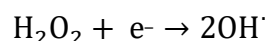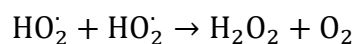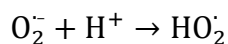### 1.4.4.2b   Photocatalytic degradation of dyes

Degradation of organic dye pollutants by photocatalysis is another promising solution for wastewater treatment [112]. Photocatalysis refers to the acceleration of a reaction by a photocatalyst in the presence of photon or light [113]. In an ideal photocatalytic reaction, organic pollutants are mineralized into CO$_2$, H$_2$O and mineral acids and reactive oxidizing species such as air or oxygen [114, 115]. The steps involved in this process are mentioned below:

(i)   When the photocatalyst is subjected to light irradiation, photons with energies equal to or higher than the band gap of the photocatalyst excite electrons from the valence band (VB) to the conduction band (CB), thereby creating electron (e$^-$)-hole (h$^+$) pairs.
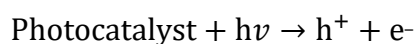
$$Photocatalyst + h\nu \rightarrow h^+ + e^-$$

(ii)   H$_2$O molecules in the reaction medium combine with the h$^+$ in the VB and generates OH· radicals. Simultaneously, the adsorbed O$_2$ molecule on the photocatalyst surface form superoxide radicals (O$_2^{-}$) by combining with the e$^-$ in the CB. The O$_2^{-}$ radicals again combine with H$^+$ ions and generates H$_2$O· radicals, which further combine with another H$_2$O· radical resulting in the formation of H$_2$O$_2$. This *in situ* generated H$_2$O$_2$ finally forms the oxidizing species, i.e., OH· radicals.
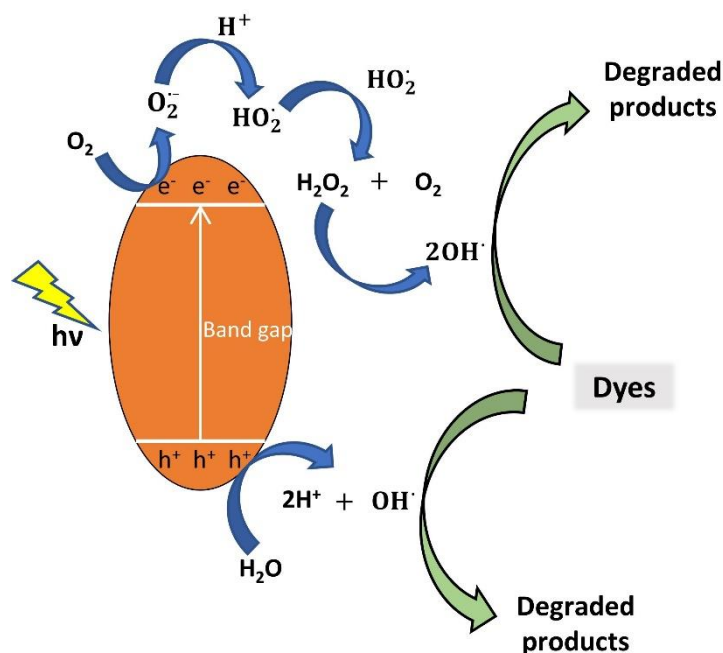
$$2H_2O + h^+ \rightarrow 2OH^· + 2H^+$$
$$O_2 + e^- \rightarrow O_2^{-}$$

$$O_2^{\cdot-} + H^+ \rightarrow HO_2^{\cdot}$$

$$HO_2^{\cdot} + HO_2^{\cdot} \rightarrow H_2O_2 + O_2$$

$$H_2O_2 + e- \rightarrow 2OH^{\cdot}$$

(iii)   The OH· radicals degrade the organic dye pollutants into degraded products.

$$OH^{\cdot} + Organic\ pollutants \rightarrow Degraded\ products$$

The possible mechanism for the photodegradation of organic dye pollutants is schematically represented in Scheme 1.5.

Scheme 1.5 Schematic diagram of the proposed mechanism for photocatalytic degradation of dyes.

The activity of a photocatalyst mainly depends upon its ability to generate electron (e^-)-hole (h^+) pairs [116]. Numerous literature reports reveal the use of various metal oxides as effective photocatalyst for degradation of dyes due to their ability to create charge carriers during light irradiation [117]. Aljaafari [118] synthesized ZnO nanosheets with a tunable thickness ranging from 20-50 nm using a microwave-assisted hydrothermal-based method. The ZnO nanosheets were employed for the photodegradation of methyl red (MR) under UV light. It was observed that the degradation performance is enhanced with decreasing thickness of the nanosheets, which could be explained based on the increasing surface area. Kale *et al.* [119] reported the photodegradation of methylene blue (MB) under sunlight irradiation using Cu-doped zinc oxide (Cu–ZnO) nanostructure with varying Cu doping (2, 4 and 6%). They

observed that the photocatalytic activity was highest for 4% doped Cu-ZnO as compared to ZnO and 2% and 6% Cu–ZnO nanostructure. The improved activity was attributed to better separation of photogenerated e^--h^+ pairs due to optimized doping in ZnO and the formation of ZnO–CuO heterojunction. Alharthi and co-workers [120] demonstrated the photocatalytic degradation of MB under both UV and sunlight irradiation using Gd/N co-doped ZnO nanoparticles. The Gd/N ZnO exhibited better degradation efficiency compared to ZnO, Gd/ZnO and N/ZnO photocatalysts and the results are presented in Figure 1.9. The better activity of the doped nanoparticles compared to pure ZnO was attributed to the improved light absorption ability and destruction of charge carriers' recombination.
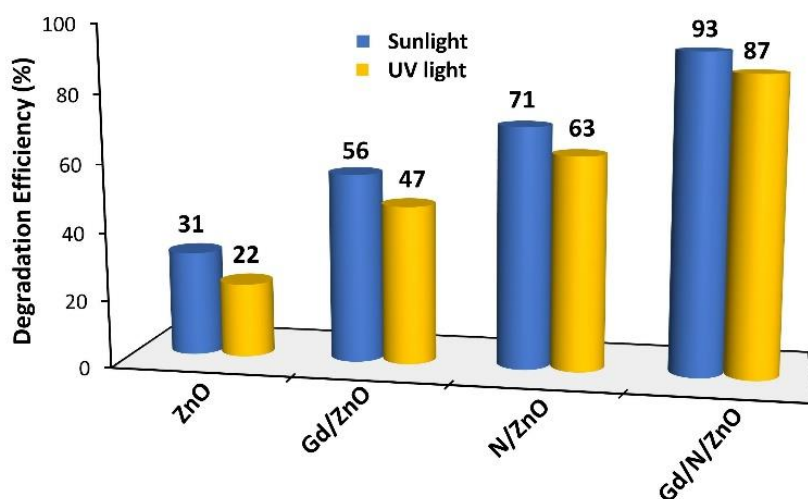
Figure 1.9 Photocatalytic degradation of methylene blue over ZnO, Gd/ZnO, N/ZnO and Gd/N ZnO.

Tuan *et al.* [121] ZnO/reduced graphene oxide (ZnO/rGO) nanocomposites with different graphene oxide concentrations (4, 6 and 10%) for the photocatalytic degradation of MB dye under visible light irradiation. It was observed that the photocatalytic activity of ZnO/rGO nanocomposites were superior to that of pure ZnO. The photocatalytic efficiency was found to increase with increasing GO concentration and the results are shown in Figure 1.10.

Figure 1.10 Photocatalytic degradation of methylene blue over ZnO/rGO nanocomposites with varying GO concentrations.
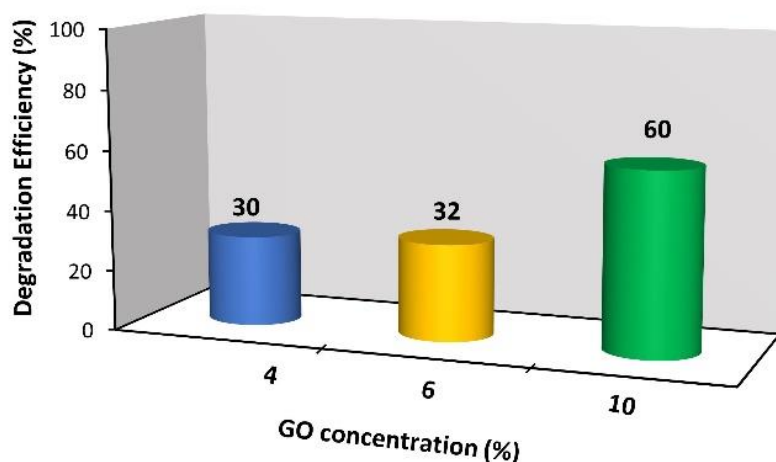
This increase in photocatalytic efficiency is attributable to enhanced dye absorption and effective charge transfer and charge separation in the ZnO/rGO nanocomposites.

1.5 Objectives of the present work

After going through the extensive literature survey as described above, the following objectives have been set for the present research work:

(i)   To synthesize and characterize ZnO and SnO$_2$ nanocatalysts for Friedel-Crafts acylation reaction.

(ii) To synthesize and characterize ZnO and SnO$_2$ supported on modified SBA-15 mesoporous silica for Friedel-Crafts acylation reaction.

(iii) Evaluation of the activity of SnO$_2$ nanostructures towards adsorptive removal of organic pollutants from aqueous solution.

(iv) To develop Cu-doped ZnO supported on reduced graphene oxide for photocatalytic degradation of organic pollutants.

REFERENCES

[1]   Parisi, C., Vigani, M., and Rodríguez-Cerezo, E. Agricultural nanotechnologies: What are the current possibilities? *Nano Today*, 10(2):124–127, 2015.

[2]   Patkar, N. B., Sharan, M., and Twain, M. Did nanotechnology flourish during the Roman empire and medieval periods? In Sharon, M., editor, *History of Nanotechnology: From Pre-Historic to Modern Times*, pages 113–140, ISBN:9781119460084. Scrivener Publishing, Wiley, 2019.

[3]   Feynman, R. P. There's plenty of room at the bottom. *Engineering and Science*, 23:22–36, 1960.

[4]   Moosa, A. A. *Nanotechnology: Principles and Applications*. Dar Dejlah Publishers & Distributors. 2011.

[5]   Taniguchi, N. On the basic concept of 'nano-technology'. In *International Conference on Production Engineering Japan Society of Precision Engineering*, pages 18–23, Tokyo, Japan, 1974.

[6]   Johnson, R. L. *Nanotechnology*. Lerner Publications, 2006.

[7]   Drexler, K. E. *Engines of creation: The coming Era of Nanotechnology*. Doubleday, New York, 1986.

[8]   Schummer, J. *Interdisciplinary Issues in Nanoscale Research.* Cambridge Scholars Publishing, 2004.

[9]   Iijima, S. Helical microtubules of graphitic carbon. *Nature,* 354(6348):56–58, 1991.

[10]   Curl, R. F., Kroto, H. W., and Smalley, R. E. Nobel prize in chemistry for 1996. *South African Journal of Chemistry-Suid-Afrikaanse Tydskrif Vir Chemie*, 50:102–105, 1997.

[11]   Singh, S. Arkoti, N. K., Verma, V., and Pal, K. Nanomaterials and their distinguishing features. In *Nanomaterials for Advanced Technologies,* pages 1–18, ISBN:978-981-19-1383-9. Springer, Singapore, 2022.

[12]   Trotta, F. and Mele, A. Nanomaterials: Classification and properties. In *Nanosponges: Synthesis and Applications*, ISBN:9783527341009. Wiley, London, 2019.

[13]   Baig, N., Kammakakam, I. and and Falath, W. Nanomaterials: A review of synthesis methods, properties, recent progress, and challenges. *Materials Advances*, 2(6):1821–1871, 2021.

[14] Lee, J. and Ko, S. H. Fundamentals of hierarchical nanostructures. In *Hierarchical Nanostructures for Energy Devices*, pages 7-25, ISBN:978-1-84973-628-2. Royal Society of Chemistry, 2014.

[15] Cao, G. *Nanostructures and Nanomaterials: Synthesis, Properties and Applications.* Imperial College Press, 2004.

[16] Barhoum, A., García-Betancourt, M. L., Jeevanandam, J., Hussien, E. A., Mekkawy, S. A., Mostafa, M., Omran, M. M., Abdalla, S. M. and Bechelany, M. Review on natural, incidental, bioinspired, and engineered nanomaterials: History, definitions, classifications, synthesis, properties, market, toxicities, risks, and regulations. *Nanomaterials*, 12:177, 2022.

[17] Wang, S., Zhou, L., Zheng, Y., Li, L., Wu, C., Yang, H., Huang, M., and An, X. Synthesis and biocompatibility of two-dimensional biomaterials. *Colloids and Surfaces A,* 583:124004, 2019.

[18] Hu, T., Mei, X., Wang, Y., Weng, X., Liang, R., and Wei, M. Two-dimensional nanomaterials: Fascinating materials in biomedical field. *Science Bulletin*, 64(22):1707–1727, 2019.

[19] Madkour, L. H. Classification of nanostructured materials. In Madkour, L. F., editor, *Nanoelectronic Materials*, pages 269–307, ISBN:978-3-030-21620-7. Springer, 2019.

[20] Mandal, A. and Ray Banerjee, E. Introduction to nanoscience, nanotechnology and nanoparticles. In Banerjee, E. R., editor, *Nanomaterials and Biomedicine,* pages 1–39, ISBN:978-981-15-5273-1. Springer, 2022.

[21] Talebian, S., Rodrigues, T., Das Neves, J., Sarmento, B., Langer, R., and Conde, J. Facts and figures on materials science and nanotechnology progress and investment. *ACS Nano*, 15(10):15940–15952, 2021.

[22] Bhatia, T., Novel nanomaterials in forensic investigations: A review. *Materials Today Proceedings*, 50:1071–1079, 2022.

[23] Henrich, V. E. and Cox, P.A. *The Surface Science of Metal Oxides*. Cambridge University Press, 1996.

[24] Védrine, J. C. Heterogeneous catalysis on metal oxides. *Catalysts*, 7(11):341, 2017.

[25] Fernandez-Garcia, M., Martinez-Arias, A., Hanson, J. C., and Rodriguez, J. A. Nanostructured oxides in chemistry: Characterization and properties. *Chemical Reviews*, 104(9):4063–4104, 2004.

[26] Arora, A. K. Metal/mixed metal oxides and their applications as sensors: A review. *Asian Journal of Research in Chemistry*, 11(2):497–504, 2018.

[27] Dey, K. K. and Srivastava, A. K. Metal oxide nanomaterials: An overview. In Srivastava, A. K., editor, *Oxide Nanostructures: Growth, Microstructures, and Properties*, pages 1–77, ISBN:9780429071386. Pan Stanford Publishing Pte. Ltd, 2009.

[28] Vaishampayan, M. V. *Synthesis characterization and applications of undoped and doped SnO$_2$ and ZnO nanostructures.* PhD thesis, Department of Chemistry, Savitribai Phule Pune University, India, 2011.

[29] Rodnyi, P. A. and Khodyuk, I. V. Optical and luminescence properties of zinc oxide. *Optics and Spectroscopy*, 111(5):776–785, 2011.

[30] Samanta, A., Goswami, M. N., and Mahapatra, P. K. Magnetic and electric properties of Ni-doped ZnO nanoparticles exhibit diluted magnetic semiconductor in nature. *Journal of alloys and compounds*, 730:399–407, 2018.

[31] Das, S. and Jayaraman, V. SnO$_2$: A comprehensive review on structures and gas sensors. *Progress in Materials Science*, 66:112–255, 2014.

[32] Sharma, D. K., Shukla, S., Sharma, K. K., and Kumar, V. A review on ZnO: Fundamental properties and applications. *Materials Today: Proceedings*, 49:3028–3035, 2022.

[33] Sun, Y., Chen, L., Bao, Y., Zhang, Y., Wang, J., Fu, M., Wu, J., and Ye, D. The applications of morphology controlled ZnO in catalysis. *Catalysts*, 6(12):188, 2016.

[34] Ani, I. J., Akpan, U. G., Olutoye, M. A., and Hameed, B. H. Photocatalytic degradation of pollutants in petroleum refinery wastewater by TiO$_2$-and ZnO-based photocatalysts: Recent development. *Journal of Cleaner Production*, 205:930–954, 2018.

[35] Liu, J., Wang, Y., Ma, J., Peng, Y., and Wang, A. A review on bidirectional analogies between the photocatalysis and antibacterial properties of ZnO. *Journal of Alloys and Compounds*, 783:898–918, 2019.

[36]   Schneider, S. L. and Lim, H. W. A review of inorganic UV filters zinc oxide and titanium dioxide. *Photodermatology, Photoimmunology & Photomedicine*, 35(6):442–446, 2019.

[37]   Jiang, Q., Zhang, X., and You, J. SnO_2: A wonderful electron transport layer for perovskite solar cells. *Small*, 14(31):1801154, 2018.

[38]   Bejtka, K., Zeng, J., Sacco, A., Castellino, M., Hernández, S., Farkhondehfal, M. A., Savino, U., Ansaloni, S., Pirri, C. F., and Chiodoni, A. Chainlike mesoporous SnO_2 as a well-performing catalyst for electrochemical CO_2 reduction. *ACS Applied Energy Materials*, 2(5):3081–3091, 2019.

[39]   Elger, A. K. and Hess, C. Elucidating the mechanism of working SnO_2 gas sensors using combined operando UV/Vis, Raman, and IR spectroscopy. *Angewandte Chemie International Edition*, 58(42):15057–15061, 2019.

[40]   Tan, L., Hu, R., Zhang, H., Lan, X., Liu, J., Wang, H., Yuan, B., and Zhu, M. Subzero temperature promotes stable lithium storage in SnO_2. *Energy Storage Materials*, 36:242–250, 2021.

[41]   Xu, L. H., Patil, D. S., Yang, J., and Xiao, J. Metal oxide nanostructures: Synthesis, properties, and applications. *Journal of Nanotechnology*, 2015: 135715, 2015.

[42]   Nunes, D., Pimentel, A., Santos, L., Barquinha, P., Pereira, L., Fortunato, E., and Martins, R. *Metal Oxide Nanostructures: Synthesis, Properties and Applications*. Elsevier, 2018.

[43]   Reddy, B. M., Bharali, P., and Saikia, P. A comprehensive overview on synthesis techniques of nanostructured oxides. In Malik, A. and Rawat, R. J., editors, *New Nanotechniques*, pages 243–276. Nova Science Publishers, New York, USA, 2009.

[44]   Baig, N., Kammakakam, I., and Falath, W. Nanomaterials: A review of synthesis methods, properties, recent progress, and challenges. *Materials Advances*, 2(6):1821–1871, 2021.

[45]   Li, J., Wu, Q., and Wu, J. Synthesis of nanoparticles via solvothermal and hydrothermal methods. In *Handbook of Nanoparticles,* pages 295–328. Springer, Cham, 2016.

[46]   Feng, S. H. and Li, G. H. Hydrothermal and solvothermal syntheses. In *Modern Inorganic Synthetic Chemistry,* pages 73–104. Elsevier, 2017.

[47]   Rane, A. V., Kanny, K., Abitha, V. K., and Thomas, S. Methods for synthesis of nanoparticles and fabrication of nanocomposites. In *Synthesis of Inorganic Nanomaterials,* pages 121–139. Woodhead Publishing, 2018.

[48]   Schäf, O., Ghobarkar, H., and Knauth, P. Hydrothermal synthesis of nanomaterials. In Knauth, P. and Schoonman, J., editors, *Nanostructured Materials: Selected Synthesis Methods, Properties and Applications*, pages 23–42. Kluwer Academic Publishers, Boston, 2002.

[49]   Sarkar, S., Guibal, E., Quignard, F., and Sengupta, A. K. Polymer-supported metals and metal oxide nanoparticles: Synthesis, characterization, and applications. *Journal of Nanoparticle Research*, 14(2):1–24, 2012.

[50]   Biswas, S., Pal, A., and Pal, T. Supported metal and metal oxide particles with proximity effect for catalysis. *RSC Advances*, 10(58):35449–35472, 2020.

[51]   Davodi, F., Mühlhausen, E., Tavakkoli, M., Sainio, J., Jiang, H., Gökce, B., Marzun, G., and Kallio, T. Catalyst support effect on the activity and durability of magnetic nanoparticles: Toward design of advanced electrocatalyst for full water splitting. *ACS Applied Materials & Interfaces*, 10(37):31300–31311, 2018.

[52]   Medhi, R., Marquez, M. D., and Lee, T. R. Visible-light-active doped metal oxide nanoparticles: Review of their synthesis, properties, and applications. *ACS Applied Nano Materials*, 3(7):6156–6185, 2020.

[53]   Pasang, T., Namratha, K., Parvin, T., Ranganathaiah, C., and Byrappa, K. Tuning of band gap in TiO_2 and ZnO nanoparticles by selective doping for photocatalytic applications. *Materials Research Innovations*, 19(1):73–80, 2015.

[54]   Huang, F., Yan, A., and Zhao, H. Influences of doping on photocatalytic properties of TiO_2 photocatalyst. In Cao, W., editor, *Semiconductor Photocatalysis: Materials, Mechanisms and Applications*, pages 31–80. InTech, Croatia, 2016.

[55]   Samadi, M., Zirak, M., Naseri, A., Khorashadizade, E., and Moshfegh, A. Z. Recent progress on doped ZnO nanostructures for visible-light photocatalysis. *Thin Solid Films*, 605:2–19, 2016.

[56]   Iqbal, J., Shah, N. S., Khan, Z. U. H., Rizwan, M., Murtaza, B., Jamil, F., Shah, A., Ullah, A., Nazzal, Y., and Howari, F. Visible light driven doped CeO_2 for the

treatment of pharmaceuticals in wastewater: A review. *Journal of Water Process Engineering*, 49:103130, 2022.

[57] Liao, C., Li, Y., and Tjong, S. C. Visible-light active titanium dioxide nanomaterials with bactericidal properties. *Nanomaterials*, 10(1):124, 2020.

[58] Das, G. S., Bhatnagar, A., Yli-Pirilä, P., Tripathi, K. M., and Kim, T. Sustainable nitrogen-doped functionalized graphene nanosheets for visible-light-induced photocatalytic water splitting. *Chemical Communications*, 56(51):6953–6956, 2020.

[59] Karthikeyan, C., Arunachalam, P., Ramachandran, K., Al-Mayouf, A. M., and Karuppuchamy, S. Recent advances in semiconductor metal oxides with enhanced methods for solar photocatalytic applications. *Journal of Alloys and Compounds*, 828:154281, 2020.

[60] Shao, G. Red shift in manganese-and iron-doped TiO_2: A DFT+U analysis. *The Journal of Physical Chemistry C*, 113(16):6800–6808, 2009.

[61] Mondal, A., Aziz, S. T., Potbhare, A. K., Mondal, S., Lambat, T. L., Chaudhary, R. G., and Abdala, A. A. Applications of metal/metal oxides nanoparticles in organic transformations. *Materials Research*, 83:134–156, 2020.

[62] Wu, X., Xu, X., Guo, C., and Zeng, H. Metal oxide heterostructures for water purification. *Journal of Nanomaterials*, 2014:603096, 2014.

[63] Huang, A., He, Y., Zhou, Y., Zhou, Y., Yang, Y., Zhang, J., Luo, L., Mao, Q., Hou, D., and Yang, J. A review of recent applications of porous metals and metal oxide in energy storage, sensing and catalysis. *Journal of Materials Science*, 54(2):949–973, 2019.

[64] Korotcenkov, G. *Metal Oxide-Based Nanostructured Electrocatalysts for Fuel Cells, Electrolyzers, and Metal-Air Batteries*. Elsevier, 2021.

[65] Kumar, P., Tomar, V., Kumar, D., Joshi, R. K., and Nemiwal, M. Magnetically active iron oxide nanoparticles for catalysis of organic transformations: A review. *Tetrahedron*, 106–107:132641, 2022.

[66] Chng, L. L., Erathodiyil, N., and Ying, J. Y. Nanostructured catalysts for organic transformations. *Accounts of Chemical Research*, 46(8):1825–1837, 2013.

[67] Ciriminna, R. and Pagliaro, M. Green chemistry in the fine chemicals and pharmaceutical industries. *Organic Process Research & Development*, 17(12):1479–1484, 2013.

[68]   Gavriilidis, A., Constantinou, A., Hellgardt, K., Hii, K. K. M., Hutchings, G. J., Brett, G. L., Kuhn, S., and Marsden, S. P. Aerobic oxidations in flow: Opportunities for the fine chemicals and pharmaceuticals industries. *Reaction Chemistry & Engineering*, 1(6):595–612, 2016.

[69]   Pan, C., Jia, X., and Cheng, J. Transition-metal-catalyzed synthesis of aromatic ketones via direct CH bond activation. *Synthesis*, 44(05):677–685, 2012.

[70]   Alamry, K. A., Saleh, T. S., Mekky, A. E., and Hussein, M. A. Ultrasound assisted microencapsulation of zinc triflate in polyethersulfone as an efficient regioselective catalyst for Friedel-Crafts acylation reaction. *Polymer*, 189:122123, 2020.

[71]   Gao, G., Zhao, Q., Yang, C., and Jiang, T. *p*-Toluenesulfonic acid functionalized imidazole ionic liquids encapsulated into bismuth SBA-16 as high-efficiency catalysts for Friedel–Crafts acylation reaction. *Dalton Transactions*, 50(17):5871–5882, 2021.

[72]   Sunke, R., Nallapati, S. B., Kumar, J. S., Kumar, K. S., and Pal, M. Use of $AlCl_3$ in Friedel Crafts arylation type reactions and beyond: An overview on the development of unique methodologies leading to N-heteroarenes. *Organic & Biomolecular Chemistry*, 15(19):4042–4057, 2017.

[73]   Castaldi, M., Baratella, M., Gaboardi, M., Castaldi, G., and Giovenzana, G. B. An efficient and scalable synthesis of fexofenadine hydrochloride. *ChemistrySelect*, 4(1):428–431, 2019.

[74]   Sartori, G., Maggi, R., and Santacroce, V. *Catalytic Friedel–Crafts Acylation Reactions*, pages 59–82. John Wiley & Sons, Inc: Hoboken, 2015.

[75]   Hattori, H. and Ono, Y. Catalysts and catalysis for acid–base reactions. In *Metal Oxides in Heterogeneous Catalysis*, pages 133–209. Elsevier, 2018.

[76]   Sartori, G. and Maggi, R. Use of solid catalysts in Friedel-Crafts acylation reactions. *Chemical Reviews*, 106:1077–1104, 2006.

[77]   Kangani, C. O. and Day, B. W. Mild, efficient Friedel-Crafts acylations from carboxylic acids using cyanuric chloride and $AlCl_3$. *Organic Letters*, 10(13):2645–2648, 2008.

[78]   Yang, X., Yasukawa, T., Yamashita, Y., and Kobayashi, S. Development of trifluoromethanesulfonic acid-immobilized nitrogen-doped carbon-incarcerated

niobia nanoparticle catalysts for Friedel–Crafts acylation. *The Journal of Organic Chemistry*, 86(21):15800–15806, 2021.

[79] Saikia, S., Devi, R., Gogoi, P., Saikia, L., Choudary, B. M., Raja, T., Deka, P., and Deka, R. C. Regioselective Friedel–Crafts acylation reaction using single crystalline and ultrathin nanosheet assembly of scrutinyite-SnO_2. *ACS Omega*, 7(36):32225–32237, 2022.

[80] Raula, M., Rashid, M. H., Paira, T. K., Dinda, E., and Mandal, T. K. Ascorbate-assisted growth of hierarchical ZnO nanostructures: Sphere, spindle, and flower and their catalytic properties. *Langmuir*, 26(11):8769–8782, 2010.

[81] Houssini, I., Harrad, M. A., Boualy, B., Ouahrouch, A., Loughzail, M., AitAli, M., and Karim, A. Development of a sustainable and solventless Friedel-Crafts acylation reaction of an aromatic natural product "Ar-Himachalene" over nanostructured ZnO as a new catalyst. *Chemistry and Materials Research*, 6(3):1–6, 2014.

[82] Hoseini, S. J., Nasrabadi, H., Azizi, M., Beni, A. S., and Khalifeh, R. Fe_3O_4 nanoparticles as an efficient and magnetically recoverable catalyst for Friedel-Crafts acylation reaction in solvent-free conditions. *Synthetic Communications*, 43:1683–1691, 2013.

[83] Mu, M., Chen, L., Liu, Y., Fang, W., and Li, Y. An efficient Fe_2O_3/HY catalyst for Friedel-Crafts acylation of m-xylene with benzoyl chloride. *RSC Advances*, 4:36951–36958, 2014.

[84] Reddy, K. R., Venkanna, D., Kantam, M. L., Bhargava, S. K., and Srinivasu, P. SnO_2−SiO_2 mesoporous composite: A very active catalyst for regioselective synthesis of aromatic ketones with unusual catalytic behavior. *Industrial & Engineering Chemistry Research*, 54:7005−7013, 2015.

[85] Rezaei, S. J. T., Nabid, M. R., Hosseini, S. Z., and Abedi, M. Polyaniline-supported zinc oxide (ZnO) nanoparticles: An active and stable heterogeneous catalyst for the Friedel-Crafts acylation reaction. *Synthetic Communications*, 42:1432–1444, 2012.

[86] Doan, T. L., Dao, T. Q., Tran, H. N., Tran, P. H., and Le, T. N. An efficient combination of Zr-MOF and microwave irradiation in catalytic Lewis acid Friedel-Crafts benzoylation. *Dalton Transactions*, 45(18):7875–7880, 2016.

[87] Das, B. C., Bhowmik, D., and Chaudhuri, S. Microwave system. *Pharma Innovation*, 1(6):1–17, 2012.

[88] Loupy, A. and de la Hoz, A. *Microwaves in Organic Synthesis*. John Wiley & Sons, 2013.

[89] Kappe, C. O., Dallinger, D., and Murphree, S. S. *Practical Microwave Synthesis for Organic Chemists: Strategies, Instruments, and Protocols*. Wiley-VCH, Weinheim, Germany, 2009.

[90] Balaguer, A. M., Rumple, A. C., and Turnbull, K. Bismuth triflate catalyzed Friedel-crafts acylation of 3-phenyl-and 3-(2-carboalkoxyphenyl) sydnones under microwave irradiation. *Organic Preparations and Procedures International*, 46(4):363–369, 2014.

[91] Tran, P. H., Phung, H. Q., Duong, M. N., and Pham-Tran, N. N. Efficient microwave-assisted direct C-benzoylation of phenols and naphthols with benzoic acid catalyzed by bismuth triflate under solvent-free or ionic liquid conditions. *Tetrahedron Letters*, 58(16):1558–1563, 2017.

[92] Tran, P. H., Nguyen, H. T., Hansen, P. E., and Le, T. N. Greener Friedel-Crafts acylation using microwave-enhanced reactivity of bismuth triflate in the Friedel-Crafts benzoylation of aromatic compounds with benzoic anhydride. *ChemistrySelect*, 2(1):571–575, 2017.

[93] Nguyen, M. T. T., Le, N., Nguyen, H. T., Luong, T. D. V., Nguyen, V. K. T., Kawazoe, Y., Tran, P. H., and Pham-Tran, N. N. Mechanism of Friedel–Crafts acylation using metal triflate in deep eutectic solvents: An experimental and computational study. *ACS Omega*, 8(1):271–278, 2022.

[94] Pasha, M. A., Manjula, K., and Jayashankara, V., P. Titanium dioxide-mediated Friedel–Crafts acylation of aromatic compounds in solvent-free condition under microwave irradiation. *Synthesis and Reactivity in Inorganic and Metal-Organic Chemistry*, 36(4):321–324, 2006.

[95] Leonel, A. G., Mansur, A. A., and Mansur, H. S. Advanced functional nanostructures based on magnetic iron oxide nanomaterials for water remediation: A review. *Water Research*, 190:116693, 2021.

[96] Naseem, T. and Durrani, T. The role of some important metal oxide nanoparticles for wastewater and antibacterial applications: A review. *Environmental Chemistry and Ecotoxicology*, 3:59–75, 2021.

[97] Xu, P., Zeng, G. M., Huang, D. L., Feng, C. L., Hu, S., Zhao, M. H., Lai, C., Wei, Z., Huang, C., Xie, G. X., and Liu, Z. F. Use of iron oxide nanomaterials in wastewater treatment: A review. *Science of the Total Environment*, 424:1–10, 2012.

[98] Ismail, M., Akhtar, K., Khan, M. I., Kamal, T., Khan, M. A., Asiri, A. M., Seo, J., and Khan, S. B. Pollution, toxicity and carcinogenicity of organic dyes and their catalytic bio-remediation. *Current Pharmaceutical Design*, 25(34):3645–3663, 2019.

[99] Abdelhamid, H. N. and Mathew, A. P. Cellulose-based materials for water remediation: Adsorption, catalysis, and antifouling. *Frontiers in Chemical Engineering*, 74, 2021.

[100] Rápó, E. and Tonk, S., Factors affecting synthetic dye adsorption; desorption studies: A review of results from the last five years (2017–2021). *Molecules*, 26(17):5419, 2021.

[101] Rafatullah, M., Sulaiman, O., Hashim, R., and Ahmad, A. Adsorption of methylene blue on low-cost adsorbents: A review. *Journal of Hazardous Materials*, 177(1-3):70–80, 2010.

[102] Shahadat, M. and Isamil, S. Regeneration performance of clay-based adsorbents for the removal of industrial dyes: A review. *RSC Advances*, 8(43):24571–24587, 2018.

[103] Daud, M., Hai, A., Banat, F., Wazir, M. B., Habib, M., Bharath, G., and Al-Harthi, M. A. A review on the recent advances, challenges and future aspect of layered double hydroxides (LDH)–containing hybrids as promising adsorbents for dyes removal. *Journal of Molecular Liquids*, 288:110989, 2019.

[104] Kumar, K. Y., Muralidhara, H. B., Nayaka, Y. A., Balasubramanyam, J., and Hanumanthappa, H. Low-cost synthesis of metal oxide nanoparticles and their application in adsorption of commercial dye and heavy metal ion in aqueous solution. *Powder Technology*, 246:125–136, 2013.

[105] Gusain, R., Gupta, K., Joshi, P., and Khatri, O. P. Adsorptive removal and photocatalytic degradation of organic pollutants using metal oxides and their composites: A comprehensive review. *Advances in Colloid and Interface Science*, 272:102009, 2019.

[106] Chen, H., Chu, P. K., He, J., Hu, T., and Yang, M. Porous magnetic manganese oxide nanostructures: Synthesis and their application in water treatment. *Journal of Colloid and Interface Science*, 359(1):68–74, 2011.

[107] Wang, L., Shi, C., Pan, L., Zhang, X., and Zou, J. J. Rational design, synthesis, adsorption principles and applications of metal oxide adsorbents: A review. *Nanoscale*, 12(8):4790–4815, 2020.

[108] Abdelkader, E., Nadjia, L., and Rose-Noëlle, V. Adsorption of Congo red azo dye on nanosized SnO_2 derived from sol-gel method. *International Journal of Industrial Chemistry*, 7(1):53–70, 2016.

[109] Athira, S., Nayana, D. A., James, K. K., and Aravind, A. Adsorption studies of hydrothermally synthesized tin oxide nanoparticles. *AIP Conference Proceedings*, 2082(1):030008, 2019.

[110] Zafar, M. N., Dar, Q., Nawaz, F., Zafar, M. N., Iqbal, M., and Nazar, M. F. Effective adsorptive removal of azo dyes over spherical ZnO nanoparticles. *Journal of Materials Research and Technology*, 8(1):713–725, 2019.

[111] Verma, M., Tyagi, I., Kumar, V., Goel, S., Vaya, D., and Kim, H. Fabrication of $GO–MnO_2$ nanocomposite using hydrothermal process for cationic and anionic dyes adsorption: Kinetics, isotherm, and reusability. *Journal of Environmental Chemical Engineering*, 9(5):106045, 2021.

[112] Subhiksha, V., Kokilavani, S., and Khan, S. S. Recent advances in degradation of organic pollutant in aqueous solutions using bismuth based photocatalysts: A review. *Chemosphere*, 133228, 2021.

[113] Umar, M. and Aziz, H. A. Photocatalytic degradation of organic pollutants in water. *Organic Pollutants-Monitoring, Risk and Treatment*, 8:196–197, 2013.

[114] Lee, K. M., Lai, C. W., Ngai, K. S., and Juan, J. C. Recent developments of zinc oxide based photocatalyst in water treatment technology: A review. *Water Research*, 88:428–448, 2016.

[115] Khataee, A. R. and Kasiri, M. B. Photocatalytic degradation of organic dyes in the presence of nanostructured titanium dioxide: Influence of the chemical structure of dyes. *Journal of Molecular Catalysis A: Chemical*, 328(1–2):8–26, 2010.

[116] Balköse, D., Ribeiro, A. C. F., Haghi, A. K., Ameta, S. C., and Chakraborty, T. *Chemical Science and Engineering Technology: Perspectives on Interdisciplinary Research*. Apple Academic Press, New York, 2019.

[117] Tan, V. T. Supported-metal oxide nanoparticles-potential photocatalysts. In *Photophysics, Photochemical and Substitution Reactions-Recent Advances*. IntechOpen, 2020.

[118] Aljaafari, A. Size dependent photocatalytic activity of ZnO nanosheets for degradation of methyl red. *Frontiers in Materials*, 362, 2020.

[119] Kale, G., Arbuj, S., Kawade, U., Kadam, S., Nikam, L., and Kale, B. Paper templated synthesis of nanostructured Cu–ZnO and its enhanced photocatalytic activity under sunlight. *Journal of Materials Science: Materials in Electronics*, 30(7):7031–7042, 2019.

[120] Alanazi, H. S., Ahmad, N., and Alharthi, F. A. Synthesis of Gd/N co-doped ZnO for enhanced UV-vis and direct solar-light-driven photocatalytic degradation. *RSC Advances*, 11(17):10194–10202, 2021.

[121] Van Tuan, P., Tuong, H. B., Tan, V. T., Thu, L. H., Khoang, N. D., and Khiem, T. N. SnO_2/reduced graphene oxide nanocomposites for highly efficient photocatalytic degradation of methylene blue. *Optical Materials*, 123:111916, 2022.